Experimental study on catenary action of RC beam-column sub-assemblages

Jun Yu and **Kang Hai Tan**

Jun Yu, PhD Student, School of Civil & Environmental Engineering, Nanyang Technological University, Singapore

Kang Hai TAN, **Associate Professor**, School of Civil & Environmental Engineering, Nanyang Technological University, Singapore

ABSTRACT

Catenary action is considered as the last defense of a structure to mitigate progressive collapse, provided that the remaining structure after an initial damage can develop alternate load paths and a large deformation has occurred in the affected beams and slabs. As a result, catenary action requires high continuity and ductility of joints. To investigate whether current RC structures designed according to ACI 318-05 could develop catenary action under column removal scenarios, two one-half scaled beam-column sub-assemblages with seismic and non-seismic detailing were designed and tested to complete failure, i.e. rebar fracture. The sub-assemblage consists of two end column stubs, a two-bay beam, and one middle beam-column joint at the junction of two single-bay beams. To ensure sufficient horizontal resistance, the sizes of end columns were enlarged to be rather stiff. To simplify the boundary conditions in the first batch of tests of our ongoing project and to make the test system statically determinate, two end column stubs were supported onto two horizontal restraints and one vertical restraint to simulate the encased supports. A concentrated load was applied vertically by a hydraulic actuator on the top of the middle joint using displacement control until the whole system eventually failed. The loading rate was controlled manually to simulate quasi-static structural behavior. The study provided insight not only into catenary action of sub-assemblages, but also the performance and failure mode of the middle joints, as well as the influence of two different detailing requirements. During the whole loading history, the cross-sectional internal forces at any beam locations can be evaluated according to the measured reaction forces. Finally, a simple analytical model will be used to check the mechanism of catenary action.

Keywords: progressive collapse, catenary action, compressive arch action, flexural action

INTRODUCTION

Recent natural catastrophes and terrorism attacks have generated substantial interest in general structural integrity for buildings and the potential to mitigate progressive collapse. Based on current building codes, such as ASCE 7-05[1], EC 1-7[2], GSA 2003[3] and DoD 2005[4], the strategies for structural design to mitigate damages caused by progressive collapse can be divided into indirect and direct design methods, in which the latter method can still be categorized into specific local resistance method (or key element method) and alternate load path (ALP) method (or notional load path method). Among these methods, ALP method forms the first proposal of a quantifiable model for designing robust buildings[5]. In practice, it is used to assess the potential of progressive collapse of a structure following the notional removal of major load-bearing elements, such as columns and bearing walls[3-4]. Under a middle column removal scenario, major alternate load paths of a reinforced concrete frame consist of Vierendeel action and Catenary action, in which the latter represents the last line of defense against collapse since it can only be activated after large deformations have occurred.

Compared with experimental studies on catenary action of steel structures, very limited experimental data[6-9] exists as the basis of assessing catenary action of reinforced concrete structures. This paper shows an experimental study on catenary action of two one-half scaled simplified RC beam-column sub-assemblages designed in accordance with ACI 318-05[10], with seismic and non-seismic detailing, respectively. The test results will be demonstrated at structure, section and fiber (i.e. reinforcing steel) levels. Finally a simple analytical model is also conducted to compare with test results.

DESCRIPTION OF TEST SPECIMENS

For a multi-bay frame, the comparison of bending moment diagram under gravity load before and after a middle column is removed is shown in Fig.1. It can be found that the so-called two-bay beams and joints above the removed column become the most crucial members to redistribute vertical loads, because the bending moment at the middle of the two-bay beams reverses its direction, and increases significantly at two ends of the two-bay beams. Please note that this is static elastic analysis. In fact, compressive arch action of the two-bay beams can be mobilized due to available axial restraints at both ends to enhance its vertical load-carrying capacity[9]. If the peak capacity of compressive arch action of beams still cannot sustain the vertical load partly due to dynamic effect, catenary action will be activated with large deformations at the midspan of the two-bay beams. The test specimens were “extracted” from a perimeter multi-bay frame, since perimeter frames are more vulnerable to terrorist attacks.

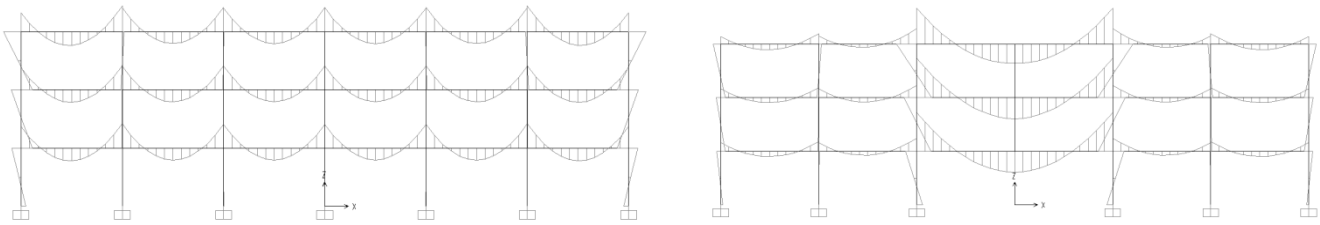

(a) Before middle column removal (b) After middle column removal

Fig.1 The comparison of bending moment diagram of a frame before and after middle column removal

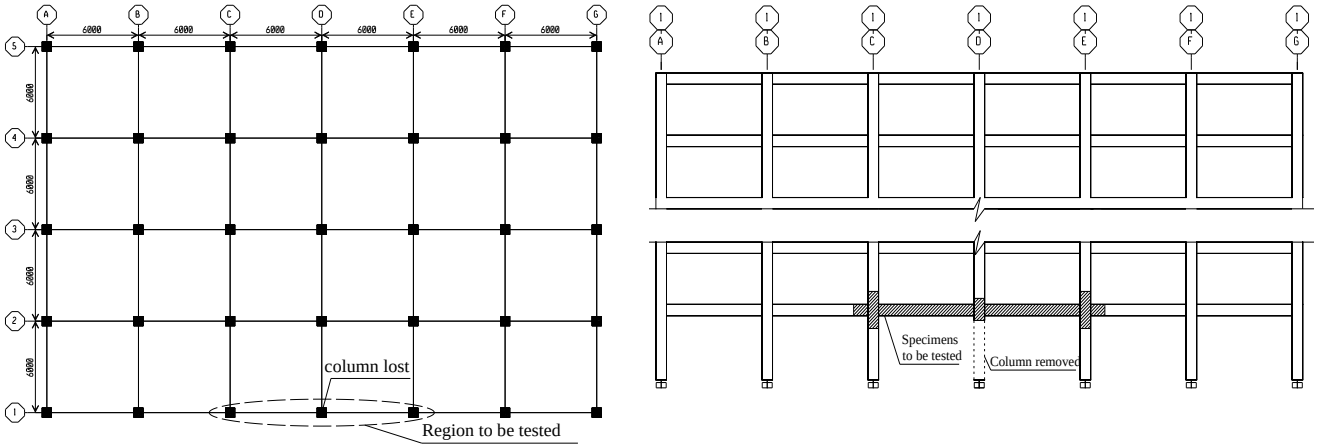

(a) The plan view of a prototype building (b) The front view of test specimens

Fig.2 The position of test specimens

The perimeter multi-bay frame is located in a 5-story comercial building, of which the ground story is 4.0 m high and the typical story is 3.3 m high. The plan view and the front view of this building are shown in Fig.2. Ideally, The test specimen should be directly taken from the shaded part of the structure, consisting of a two-bay beam, a middle joint and beam column extensions, as seen in Fig. 2(b), to consider the continuity effect of adjacent columns and beams on the directly affected two-bay beams. However, to simplify the testing, and also to provide sufficient anchorage for reinforcing steel in the two-bay beams, beam column extensions are replaced by concrete stubs with a section size larger than the actual columns. Thefore, the test specimen is referred to as a simplified beam-column sub-assemblage, which comprises a two-bay beam, a middle joint and two end column stubs.

For seimic design, it is assumed that the building is located in Site D and designed as a special moment-resisting frame. According to ASCE 7-05[1] and ACI 318-05[10], the detailing of two one-half scaled specimens is shown in Fig.3. Please note that due to symmetry of specimens, only half of specimens are shown herein. The geometry of members and material properties of the test specimens are summarized in Table 1 and Table 2, respectively. All material testing followed the corresponding standards of ASTM. To investigate the effect of splices on the development of catenary action in beams, the two bottom longitudinal

reinforcement of each specimen is spliced according to the requirments of ACI 318-05[10]. The tension splice of specimen S1 is Class B splice (i.e. equal to 1.3 times development length l_d of reinforcement) and that of specimen S2 is Class A splice (i.e. l_d).

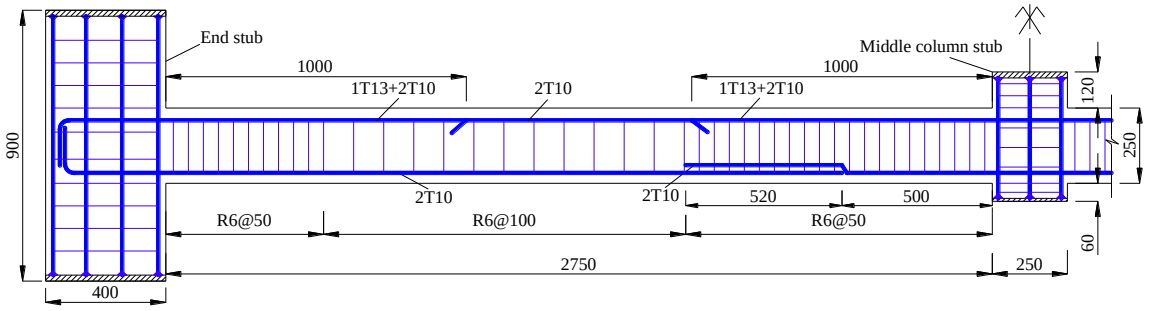

(a) Seismic specimen S1

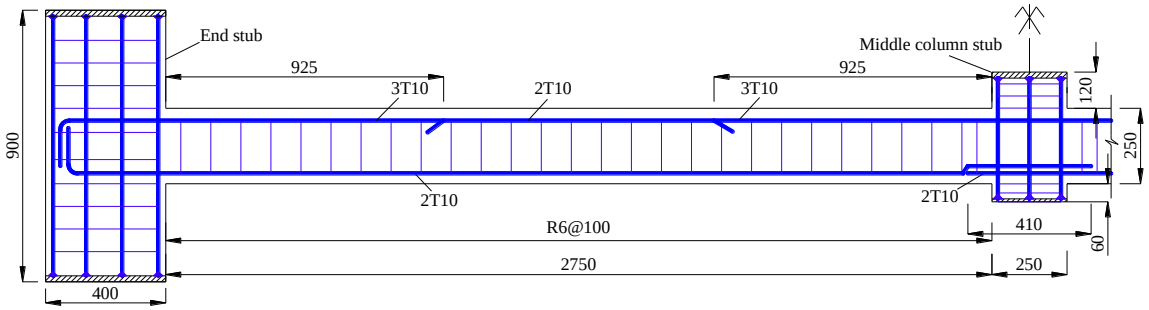

(b) Non-Seismic specimen S2

Fig.3 The detailing of simplified beam-column sub-assemblages (unit: mm)

Table 1 Specimen properties

Specimen No.	Beam size (mm)		Middle column stub size (mm)		Edge stub (mm)		Reinforcement ratio at the middle joint*	
	Depth	Width	Depth	Width	Depth	Width	Top	Bottom
S1	250	150	400	450	250	250	0.90% (1T13+2T10)	0.49% (2T10)
S2	250	150	400	450	250	250	0.73% (3T10)	0.49% (2T10)

* Concrete cover thickness is 20 mm.

Table 2 Material properties of the specimens

Tested Items		Yield strength (MPa)	Ultimate tensile strength (MPa)	Fracture strain (%)*
Longitudinal reinforcement	T10	511	731	12.32
	T13	527	640	10.76
Links	R6	310	422	14.00
Concrete (150 mm (dia.) x 300 mm (height))		Compressive strength: 31.2 MPa Splitting tensile strength: 3.2 MPa		

*All reinforcement strength is based on the nominal diameter of reinforcement and the gage length of reinforcement is 200 mm; "T" represents high-yield strength reinforcement with nominal yield strength of 460 MPa and "R" represents low-yield strength reinforcement with nominal yield strength of 250 MPa.

TEST SET UP AND INSTRUMENTATION

Fig.4 illustrates the boundary conditions and the loading method of the testing. The combination of two horizontal restraints and one vertical restraint connected to each end column stub simulates the vertical, axial and rotational restraints imposed at the beam end by the adjoining frame structure. As shown in Fig.5, at one end, two horizontal restraints were connected to the steel frame anchored to the strong floor and at the other end two horizontal restraints were connected to a thick steel plate fixed to the vertical reaction wall. Two transverse frames were used to prevent out-of-plane movement of the test specimens. Based on previous research work[11], a concentrated load was applied at the middle joint using a hydraulic actuator with a stroke length of 1000 mm. The load was applied with displacement control until the specimen totally failed by fracture of reinforcing steel.

The arrangement of the instrumentation system is shown in Fig.6. Line displacement transducers and linear variable differential transformers (LVDT) were used to measure vertical displacement along the whole beam, end movements and local rotations. Strain gages attached to reinforcement at specified sections to shed light on the variations of internal forces and the mechanisms developed in the beam, i.e. flexural action, compressive arch action and catenary action. Load cells and strain gages were used to measure reaction forces to make the test set-up statically determinate, as shown in Fig.7. Please note that the load cells used to measure vertical reaction forces were beneath the base steel plates. The applied force was measured by a built-in load cell of the actuator.

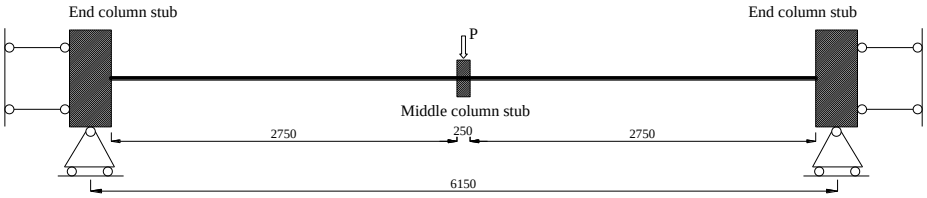

Fig.4 The concept of test set-up (unit: mm)

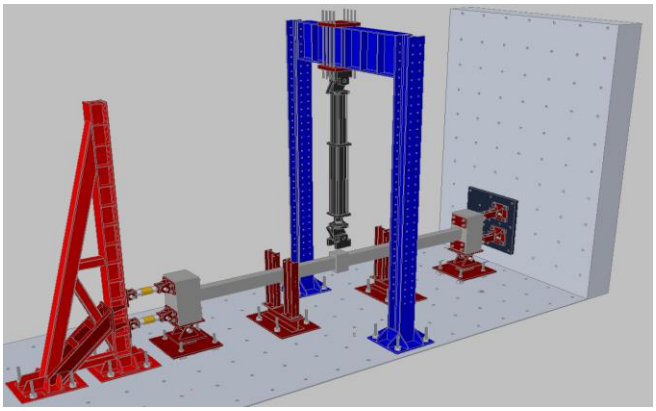

Fig. 5 Perspective view of test set-up

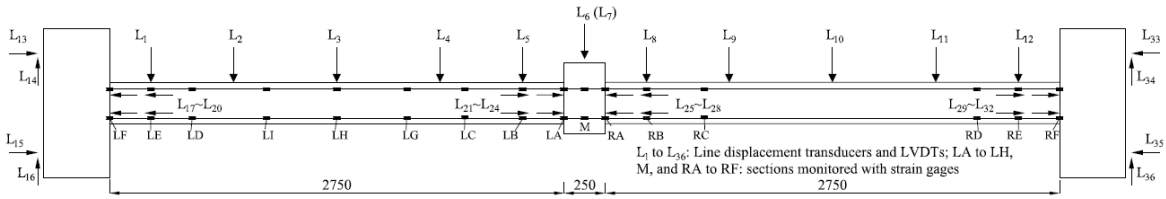

Fig.6 The layout of instrumentation

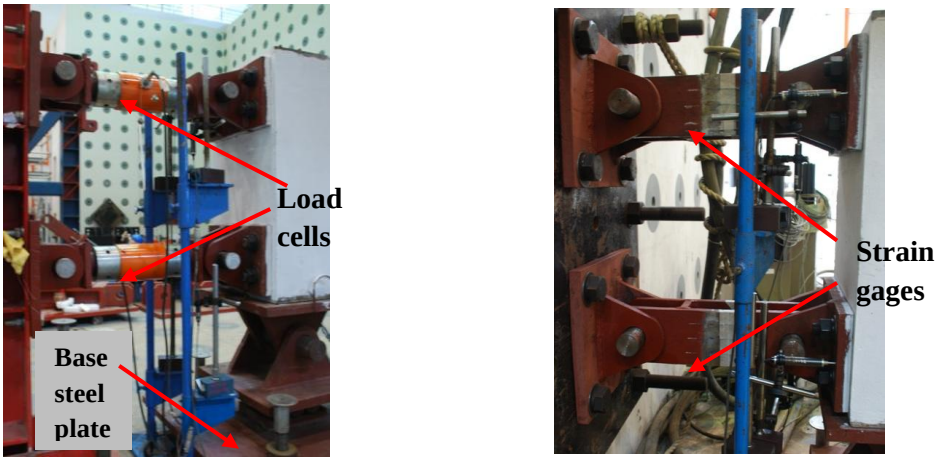

(a) using load cells (b) using strain gages

Fig.7 The methods to measure reaction forces

TEST RESULTS

The test results will be demenstrated at three levels, i.e. structrure, section and fiber (espcially for reinforcing steel). The test data herein do not take account of the effect of self-weight of specimens.

TEST RESULTS AT STRUCTURE LEVEL

The displacement of middle joint increased slowly until a top reinforcing steel bar at one end of the beams fractured. The failure mode of two spcimens were very similar, as shown in Fig.8. The specimens experienced large deformations and rotations prior to failure. The displacement of middle joints for both specimens at the end of the tests reached around 600 mm, approximately 10% of total span length (5750 mm). At failure , the rotation of one side of the middle joint was 15.5° and 16.0° for specimen with seismic and non-seismic detailing, respectively. The overall behavior of two specimens can be represented in terms of relationship of the applied load versus the middle joint displacement and the horizontal reaction force versus the middle joint displacement, as shown in Figs. 9 and 10, respectively. Please note that all the sudden reductions of the applied force in Fig.9 were caused by fracture of reinfircing steel. The values of the applied forces and displcements of critical points of the curves in Fig.8 are listed in Table 3.

Fig.8 The failure mode of the specimens

Initially, the specimens functioned as conventinal beams in flexural action. However, since the positive bending moment at the middle joint was maximum along the whole two-bay beam and the reinforcement ratio at the bottom layer of the middle joint was very light, cracks developed and spread fast near the middle joint. With the middle joint displacement increasing, compressive arch action occurred. The arch action could be identified from the magnitude of axial force larger than 10% of nominal compressive strength of beam section ($0.1f_c'A_g$=117.15 kN) which is used to define *the limit of flexural beam mechanism*, or from the measured peak capacity greater than the calculted ultimate bending capacity based on plastic hinge mechanism (without considering the effect of axial force), as shown in Table 3. After attaining the peak capacity, partly due to concrete near both joint faces crushed severely and reaching compressive softening stage, the specimen deflected more and its capacity decreased until catenary action developed and sustanined the vertical applied force.

Fig.10 shows that the decrease of axial compression was not so noticeable between 100 and 200 mm of the middle joint displacement, suggesting that at this range the descending path of the capacity was caused by snap-through phenomenon. For the specimen with seismic detailing, catenary action developed after two bottom reinforcing bars at one side of the middle column joint fractured sequentially. For the specimen with non-seismic detailing, catenary action commenced at 255 mm of the middle joint displacement and one spliced bottom bar at one side of the middle joint fractured. After that, catenary action continued to increase due to the contribution of the top reinforcement. The variation of reaction force in Fig.10 illustrates that after catenary action was mobilized, tension force started developing along the two-bay beam.

Fig.11 demonstrates the ultimate failure mode of one side of the middle joint. Concrete at the top part of the joint was completely crushed, bottom bars fractured and several wide cracks penetrated the whole beam section. Due to the lack of rotational restraint at the middle joint and non-uniformity of concrete mateterial itself, the cracks which arose at both sides of the middle joints were not symmetrical. The middle joint gradually inclined towards the side with relatively more severe cracks during the loading process, especially after the peak capacity had been attained. From Fig.11, it can be seen that the cracks of the specimen with non-seismic detailing were more severe than those of the specimen with seismic detailing. The was no splice failure obseved for both specimens. However, the occurance of longitudinal cracks at the bottom layer indicated the development of large bond stress from the middle joint to the adjacent beam. It should be noted that the confinement effect of the specimen with non-seismic detailing was poorer than that with seismic detailing. If the splice length was too short or if there was no splice, the reifnorcement would have been pulled out when subjected to axial tension. In the test, the lap spliced reinforcement finally fractured rather than being yanked out, and hence even the Class A splice could meet the continuity requirements.

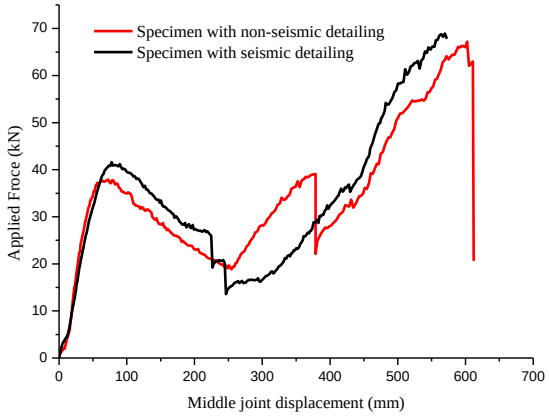

Fig. 9 The relationship of applied force to middle joint displacement

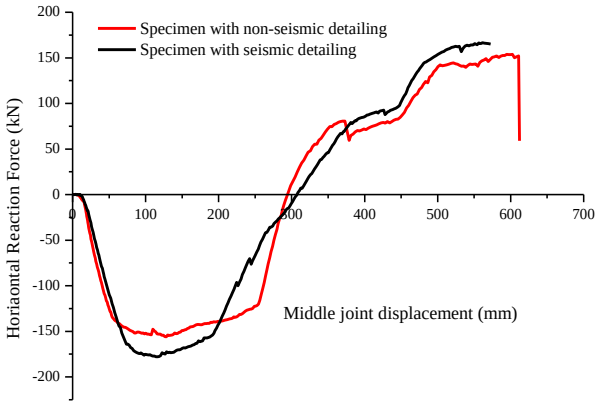

Fig. 10 The relationship of horizontal reaction force and middle joint displacement

Table 3 The value of force and displacement at critical points

Specimens	Critical displacement (mm)					Critical capacity (kN)		
	At the first Peak capacity	Capacity reversing to rise	1st rebar fracture or turn up*	2nd rebar fracture	Top rebars at beam end fracture	Calculated ultimate bending capacity	Peak capacity due to compressive arch action	Catenary action capacity
Seismic detailing	78	246	227	246	573	33.08	41.64	68.91
Non-seismic detailing	73	255	379	N.A.	612	29.02	38.38	67.63

* The rebars mentioned are located at the bottom layer of the middle joint

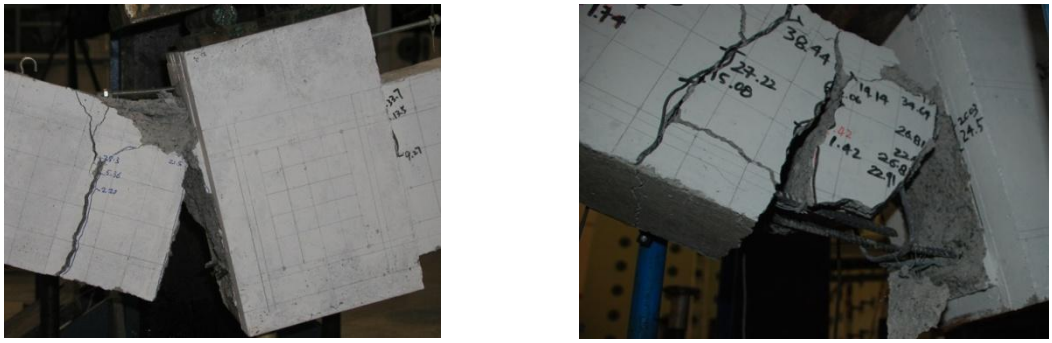

(a) the specimen with seismic detailing (b) the specimen with non-seismic detailing

Fig.11: The failure modes of one side of middle joints

(a) the specimen with seismic detailing (b) the specimen with non-seismic detailing

Fig. 12: The failure modes at beam ends

Fig.12 shows the failure modes at the beam ends. It can be seen that several cracks extensively penetrated across the whole beam section. The concrete at the soffit was severely crushed. The fracture of top reinforcement resulted in the complete separation of beam section from the column stub.

TEST RESULTS AT SECTION LEVEL

Since the positions of the neutral axis at different beam sections are different, all internal forces acting at the beam cross sections are calculated based on the geometrical center of each section. Although the deformation of the two specimens and the corresponding section rotations were very large, the variation of the axial force at all sections was not appreciably different from that of the horizontal reaction force shown in Fig.10.

From statics, the bending moments at different sections for both specimens are shown in Fig.13. For the specimen with seismic detailing, the reduction of the bending moment at the left side of the middle joint after the first peak value was due to concrete reaching compressive softening stage, and the re-ascending path was attributed to the hardening of bottom reinforcement between the 100 and 200 mm of the middle joint displacement, during which the strain of top reinforcement is relatively stable, as shown in Figs.15 (a). Similarly, for the specimen with non-seismic detailing, after concrete deteriorated, the bending moment at the joint face decreased. However, there is no obvious immediate increase, indicating that it is not efficient to mobilize the hardening of reinforcement in lap splice compared with continuous reinforcement. After the bottom reinforcement had fractured, the bending moment at the joint faces were induced by shifting of axial force to the geometric center of the sections.

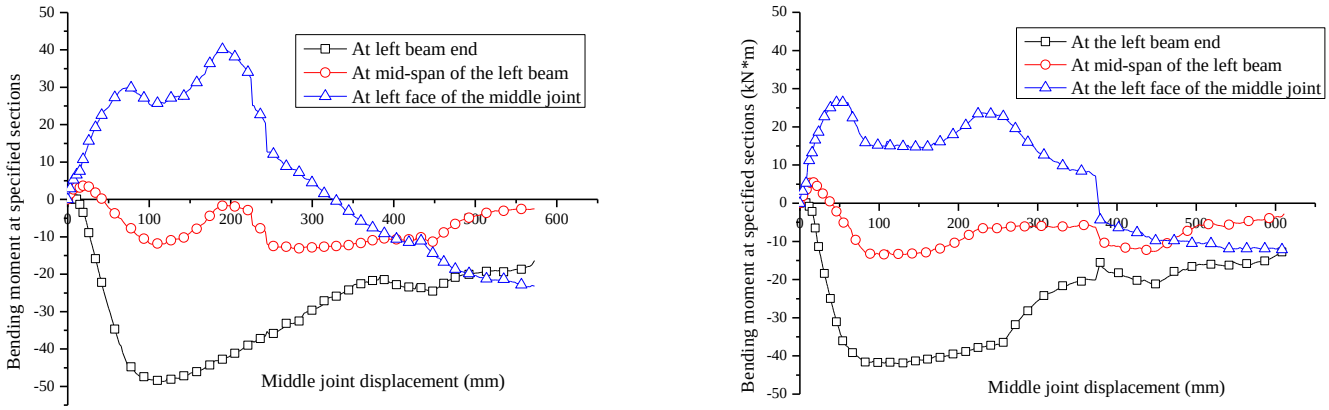

(a) Specimen with seismic detailing

(b) Specimen with non-seismic detailing

Fig.13 The variation of bending moment at different beam sections

The shear forces at different sections for both specimens are shown in Fig.14. The sign convention is that at any cut the shear force is positive if it is acting downwards to the left of the rigid body diagram and upwards to the right of the diagram. After cracks had penetrated the whole beam section, the rotations of sections at two sides of the cracks became non-continuous, resulting in non-continuous shear forces as well. For example, there is no relative rotation between the end column surface and the beam end initially, just like two sides of one section, and hence the shear forces for both sides are equal in terms of magnitude, as shown in Fig.14. With increasing the middle joint displacement, the cracks became larger and the relative rotation between two sides occurred. As a result, the shear forces at two sides of the

same section differed from each other. At the ultimate state, the magnitude of shear force is less than 10% axial tension force developed near the middle joint, suggesting that the shear force can be neglected in the calculation of the maximum capacity of catenary action.

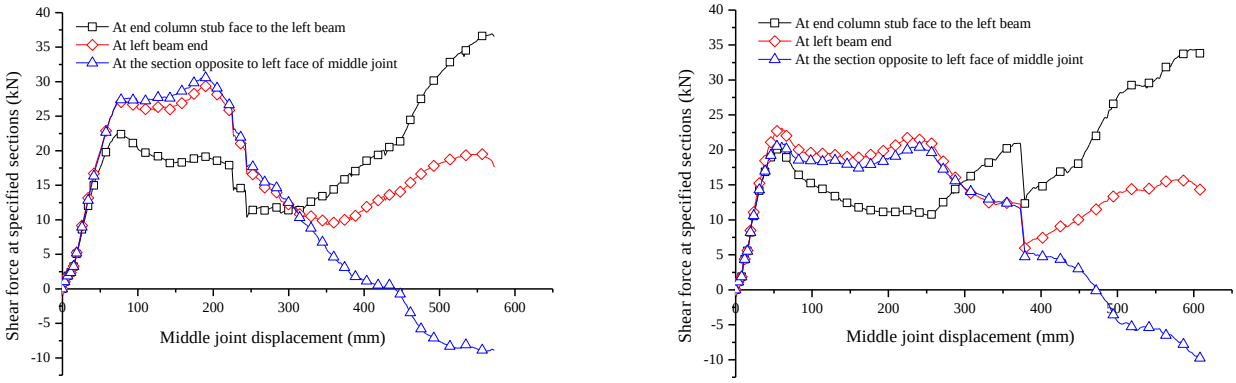

(a) Specimen with seismic detailing

(b) Specimen with non-seismic detailing

Fig.14 The variation of shear force at different sections

TEST RESULTS AT FIBER LEVEL

The strain development of reinforcing steel at the sections which were located at the high strain regions is shown in Fig.15.The yield strain of reinforcing steel is 2800μ. Fig. 15(a) shows that the strain of bottom reinforcement increased rapidly at the side of the middle joint. After experiencing large compression strain, top reinforcement reversed into tension to develop catenary action. In the test, it was also observed that yielding of top reinforcement penetrated from the joint faces to the center of the middle joint, thus reducing the bond stress along the top reinforcement due to large plastic strain. Fig. 14(d) demonstrates that even the bottom reinforcement at the beam end finally changed into tension, suggesting that the whole beam section is under tension at the ultimate stage of catenary action.

THE MECHANISM OF CATENARY ACTION

Based on test results, it can be found that during catenary action the whole beam is under tension. When the tension force is very large, even at the beam end the section is transformed into pure tension state. Once the magnitude and the orientation of the tension forces at both sides of a middle joint are known, the applied load can be estimated with a simple model, $P = 2N_t \sin\theta$, as shown in Fig.16. In the tests, θ can be measured and the axial force can be calculated based on measured reaction forces. Fig.16 shows a comparison of calculated load with applied load. Due to the lack of rotational restraint at the middle joint, the joint rotated during catenary action, resulting in the rotation of the actuator as well. This vertical component is equal to P. Therefore, the calculated load should be slightly smaller than the applied load.

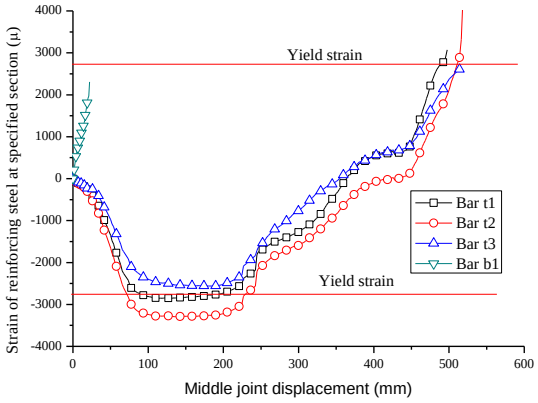

(a) Strain of reinforcement at RA section

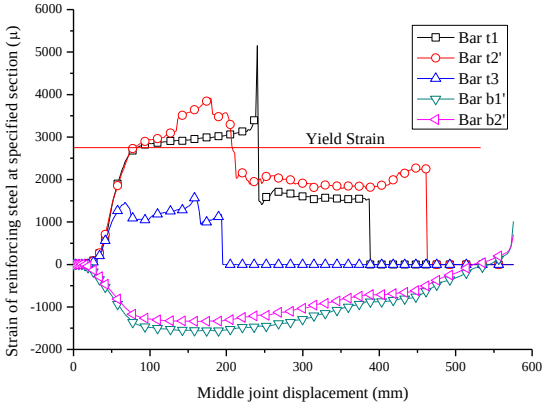

(b) Strain of reinforcement at LE section

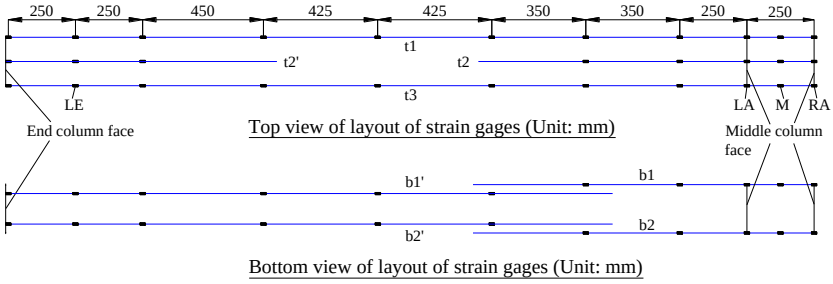

(c) The layout of strain gages

Fig. 15 The reinforcement strain at specified sections of the seismic detailing specimen

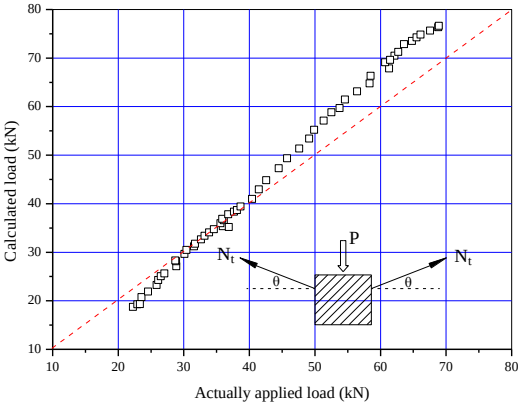

(a) For seismic detailing specimen

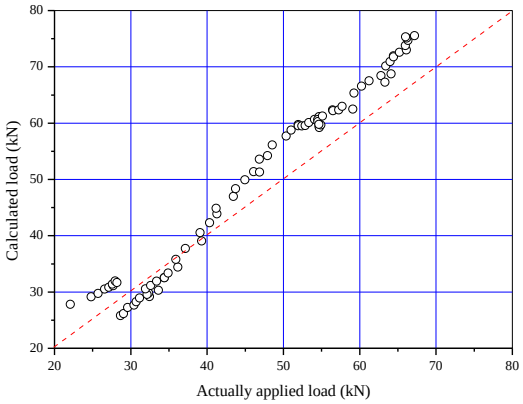

(b) For non-seismic detailing specimen

Fig.16 Comparison of calculated load with applied load during catenary action

DISCUSSIONS

The mechanism of catenary action is that axial tension along the beam sustains the applied load. Therefore, the onset of catenary action can be defined at the moment when the beam axial force changes from compression to tension[7]. However, the re-ascending of the load capacity, shown in Fig.9, occurs ahead of the axial force changing from compression to tension. Sasani and Kropelnicki[6] selected the reversing point to the re-ascending path as the start of catenary action. So far there is no clear definition for the onset of catenary action.

The bottom reinforcement at the middle joint basically did not contribute to catenary action for the specimen with seismic detailing. Before catenary action developed, they had already fractured. It is not like the test results reported by Yi, *et al*. (2008) and Su, *et al*. (2009) that bottom reinforcement at the middle joint can contribute to developing catenary action. The discrepancy is yet to be investigated.

In the simple analytical model, the calculated load is based on the measured rotation and the computed axial forces. However, it is believed that there is an intrinsic relationship between the axial force and the rotation at both sides of the middle joint, which will be studied in our future work.

SUMMARY AND CONCLUSIONS

Catenary action of two one-half scaled RC beam-column sub-assemblages under middle column removal scenario is reported in this paper. The load-deformation history of tested specimens indicates that large vertical deformations are prerequisite for catenary action to develop. The magnitude of deflections varies around one beam depth (250 mm) to 600 mm in the two tests. The capacity of catenary action is 65.5% and 76.2% higher than the peak capacity of compressive arch action for the specimen with seismic and non-seismic detailing, respectively. However, the failure of catenary action was not controlled by the fracture of top reinforcement going through the middle joint but by the fracture of top reinforcement at the beam ends. During catenary action, due to penetration of severe cracks, the sections at the beam ends and the joint faces became separated and shear forces were not continuous in terms of magnitude. Therefore, to simulate catenary action of an RC structure with FEM, an independent beam column joint model is essential. Moreover, the large axial tension force during catenary action causes the top reinforcement to yield from the outside to the inside of the middle joint, reducing bond stress tremendously.

The detailing of two specimens did not significantly affect the test results, indicating that the shear behavior of the specimens was not significant during the test and both lap splice of Class A and Class B type according to ACI 318-05 can meet the continuity requirements.

ACKNOWLEDGEMENTS

The authors gratefully acknowledge the funding provided by Defence Science & Technology Agency, Singapore.

REFERENCES

1. American Society of Civil Engineers (ASCE) . "Minimum Design Loads for Buildings and Other Structures," ASCE/SEI 7-05, American Society of Civil Engineers, Reston, Virginia, 2005.
2. Comite Europeen de Normalisation. "Eurocode 1 - Actions on structures - Part 1-7: General actions - Accidental actions. ENV 1991-2-7: 1998," 2006.
3. General Services Administration (GSA). "Progressive Collapse Analysis and Design Guidelines for New Federal Office Buildings and Major Modernization Projects," Washington, DC, 2003
4. Department of Defense (DOD). "Design of Buildings to Resist Progressive Collapse". Unified Facilities Criteria (UFC) 4-023-03, 25 January, 2005.
5. Gurley, C. R. "Progressive Collapse and Earthquake Resistance," *Practice Periodical on Structural Design and Construction*, V.13, No.1, Feburary 2008, pp. 19-23.
6. Sasani, M., and Kropelnicki, J. (2007). "Progressive collapse analysis of an RC structure," *The Structural Design of Tall and Special Buildings*. V.17, No.4, 2007, pp. 757-771.
7. Orton, S. L. "Development of a CFRP System to Provide Continuity in Existing Reinforced Concrete Buildings Vulnerable to Progressive Collapse," Austin, University of Texas. Doctor of Philosophy, 2007
8. Yi, W. J., He, Q.F., Xiao, Y., and Kunnath, S.K. "Experimental study on progressive collapse-resistant behavior of reinforced concrete frame structures," *ACI Structural Journal*, V. 105, No.4, July-August 2008, pp. 433-439.
9. Su, Y. P., Tian, Y., and Song, X.S. "Progressive collapse resistance of axially-restrained frame beams," *ACI Structural Journal*, V. 106, N.5, September-October 2009, pp. 600-607.
10. ACI Committee 318. "Building Code Requirements for Structural Concrete (ACI 318-05)," American Concrete Institute, Farmington Hills, Michigan, 2005
11. Demonceau, J. F. "Steel and composite building frames: sway response under conventional loading and development of membrane effects in beams further to an exceptional action," Faculte des Sciences Appliquees. Liege, Belgium, University of Liege. Doctor of Philosophy, 2007